Rad. and Environm. Biophys. 12, 31—39 (1975)

Analysis of PCP-Data to Determine the Fraction of Cells in the Various Phases of Cell Cycle*

Heinz Baisch, Wolfgang Göhde, and Walfried A. Linden
Institut für Biophysik und Strahlenbiologie der Universität Hamburg
and
Institut für Strahlenbiologie der Universität Münster

Received September 10, 1974/In Revised Form February 22, 1975

Summary. Mathematical models for the analysis of pulse-cytophotometric (PCP) data are described. With computer programs based on these models the fractions of cells in G_1-, S- and (G_2 + M)-phases are obtained. The methods are applied to PCP-measurements of Ehrlich ascites tumor cells, human bone marrow cells and L-929-cells in culture. The results of the L-cell experiment are compared with autoradiographic results; for both methods the duration of the various phases has been calculated. Two different mathematical models for PCP-data evaluation and the autoradiographic method yielded results agreeing within statistical error. The application of the two models on different types of DNA-histograms is discussed: One model is suitable for asynchronous cell populations with a low fraction of S-phase cells, the other can be applied for partially synchronized cells and high S-phase fractions as well.

1. Introduction

Determination of cell cycle kinetics is becoming more and more important in cancer research, medical diagnostics and therapy of malignant tumors [1, 5, 20]. The influence of chemical agents (*i.e.* cytostatic drugs) as well as irradiation is usually different in the different phases of the cell cycle [18, 19]. For studies of these drugs it is therefore useful to know the fraction of cells in the G_1-, S-, G_2- and M-phases [7, 13], especially when trying to apply a phase-specific agent to increase the tumor cell killing effect in therapy.

Cell proliferation parameters can be obtained by the well-known methods of micro-autoradiography [2, 10] and determination of mitotic index. In the last years a new method has been developed: Pulse-cytophotometry [4, 8], which is much faster than autoradiography. More than 1000 cells can be measured per second yielding a distribution of DNA-content (DNA-histogram). The DNA-histograms contain information about the fraction of cells in the different phases. To get quantitative results a mathematical analysis of PCP-data basing on two models has been evaluated. The results are compared with those obtained by autoradiography [17].

2. Materials and Methods

Ehrlich ascites tumor cells *in vivo*, human bone marrow cells and L-929-cells in culture were measured using PCP. The technique has been reported in detail previously [6, 8, 9, 17] and is only briefly described here. The cells were fixed with

* Supported by the Deutsche Forschungsgemeinschaft Bonn-Bad Godesberg.

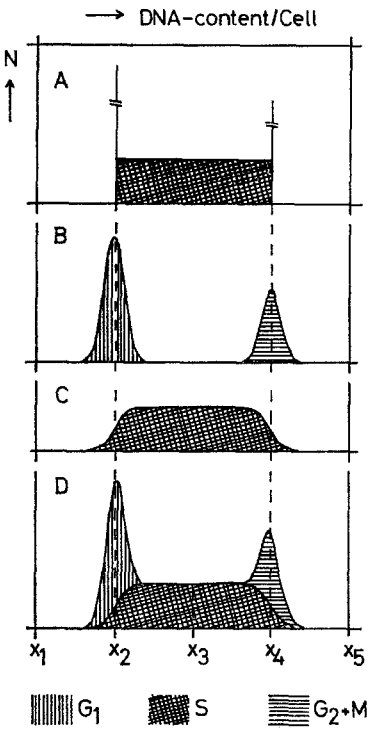

Fig. 1. Schematic representation of DNA-histograms (see text)

96% ethanol and treated with RNase and ethidium bromide, a fluorescent dye which specifically binds to DNA. The relative DNA content of about 100000 cells was measured by PCP, the DNA content being proportional to the channel number of a multi-channel analyzer. The data of each DNA-histogram were punched on paper tape for further evaluation.

3. Mathematical Analysis of PCP-Histograms

Typical experimental DNA-histograms are shown in Figs. 3 and 4. The peak at 2C represents the G_1-cells, the peak at 4C the (G_2 + M)-cells. The S-cells appear between the peaks according to their intermediate DNA-content. A quantitative determination of fractions of cells in the different phases is complicated by the overlapping of S-phase-cells with G_1- and G_2-cells. Two mathematical models are proposed here to compute fractions of cells in G_1-, S- and (G_2 + M)-phases.

Assuming an extremely homogeneous cell population and provided the PCP-measurement is absolutely exact, all G_1-cells should appear in one single channel of the DNA-histogram (in Fig. 1A at X_2). The (G_2 + M)-cells have twice as much DNA as G_1-cells and consequently should be measured in one single channel at double the G_1 channel (X_4 in Fig. 1A). The S-phase cells with intermediate DNA-content appear between X_2 and X_4. If the rate of DNA-synthesis is constant during the whole S-phase, the number of cells in all channels should be the same in a steady-state culture (see Fig. 4). For exponentially growing cultures the age distribution of cells in S-phase is a slightly decreasing function [12].

Assuming a constant rate of DNA-synthesis the number of cells entering S-phase per unit time is increasing with time. This leads to a slowly decreasing exponential function for the probability distribution of the cellular DNA contents in S as well. As can be seen from experimental DNA-histograms (Fig. 3), the decrease of the curve in S-phase is very small. Therefore it can be approximated by a parallel to the base line. Thus in Fig. 1A the S-phase is represented by the rectangle between X_2 and X_4. In real experiments there are a couple of error sources (dying, optical and electronic errors) which lead to deviations in the experimental values. Thus, even for homogenous cell populations G_1- and (G_2 + M)-phase cells yield more or less broad distributions for the measured DNA-content (Fig. 1B). The same is true for S-phase cells, but the histogram is modified only at the beginnnig (X_2) and the end (X_4) of S-phase (Fig. 1C), in the middle part the errors cancel out. So in real experiments G_1-phase is overlapping the beginning of S-phase in the histogram (Fig. 1D). As can easily be seen, the peaks of G_1 and G_2 are no longer at X_2 and X_4, respectively, but both are shifted to the center (X_3). Measured DNA-histograms look almost exactly like the constructed one in Fig. 1D (see Fig. 3). So we can take it to explain the mathematical models.

Model 1

In cell populations containing a relatively small fraction of S-phase cells the shift of G_1- and G_2-peak is only small. We neglect it and take the measured G_1-peak for X_2 and the G_2-peak for X_4. Now the number of cells in S-phase is given by the area of the rectangle:

$$S = N(X_3) \cdot (X_4 - X_2) .$$

In real experiments statistical fluctuation has to be considered, therefore it is better to replace $N(X_3)$ by a mean value (N_S) of the cell number per channel:

$$N_S = 1/(K+1) \sum_{X_i=X_3-K/2}^{X_3+K/2} N(X_i) .$$

In practice K is fixed to 4 to 10 depending on the total number of channels occupied by S-phase.

The number of cells in G_1 phase is obtained by subtracting the area of S from the total area under the curve up to channel X_3:

$$G_1 = \sum_{X_i=X_1}^{X_3} [N(X_i) \cdot \Delta X] - S/2 .$$

In the same way we get the amount of (G_2 + M)-cells:

$$G_2 + M = \sum_{X_i=X_3}^{X_5} [N(X_i) \cdot \Delta X] - S/2 .$$

According to this model the fraction of G_1-, S- and (G_2 + M)-cells is calculated by a simple computer program from the DNA-histogram data.

Model 2

The error of the above approximation is only small, provided the S-phase cell fraction is low and the proliferation is asynchronous. Under the influence of cyto-

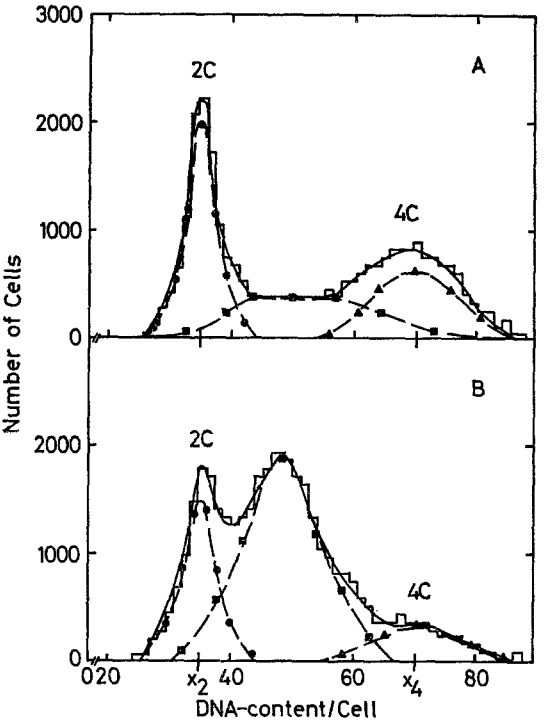

Fig. 2. Schematic representation of DNA histograms and corresponding fit-curves. The solid line represents the total fit function, broken lines are fit functions for different cell-cycle phases: G_1-phase (●), S-phase (■), (G_2 + M)-phase (▲). Part A: DNA-histogram of an asynchronous cell population, Part B: DNA-histogram of a partially synchronized cell population

static agents or ionizing radiation the cells can become partially synchronized or blocked. Treated cell populations can contain considerably higher fractions of cells in the S-phase. In model 2 this has been taken into account and this model is more accurate regarding the theoretical consideration. The mathematical model is demonstrated by Fig. 2 which shows typical experimental histograms. Part A shows the schematic drawing of a DNA-histogram from an asynchronous cell population, part B from a partially synchronized population, the synchronized fraction just passing through S-phase.

Considering the type of errors which lead to deviations of the experimental values from the real DNA-contents we can assume that the G_1- and (G_2 + M)-curves are normal distributions:

$$G_1(X) = C_1 \cdot \exp - [(X - X_2)^2/(2\,\sigma_2^2)]\,,$$
$$G_2M(X) = C_2 \cdot \exp - [(X - X_4)^2/(2\,\sigma_4^2)]\,,$$

where C_i are coefficients proportional to the total number of cells in that phase and σ_i are standard deviations.

For S-phase cells the same type of instrumental dispersion occurs as for G_1 and (G_2 + M)-cells. Thus it is reasonable to assume that the edge of the distribution

of DNA contents in S-phase at the G_1— S transition may be described by the distribution function of a normal distribution:

$$S(Z) = C_S \cdot \int_0^Z \exp\left[-(X - X_2)^2/(2\,\sigma_2^2)\right] dx\,.$$

The DNA-content of cells which have just entered S-phase differs only slightly from that of G_1-cells. Therefore, in the above formula the same variance σ_2^2 has been taken as for the G_1 normal distribution.

For $Z > (X_2 + 2\,\sigma)$ the integral becomes asymptotically constant. The coefficient C_S which is proportional to the number of cells in S is constant only for steady-state cell populations. In exponentially growing cultures the number of cells entering S-phase is increasing with time. Thus the coefficient C_S is a function of Z, which leads to the slightly decreasing function for the distribution of DNA contents of S-phase cells. The same approximation as in model 1 (S-curve parallel to base line) is made, giving constant coefficient C_S all over the S-phase. Now the coefficient C_S can easily be calculated by fitting the integral S (Z) to the experimental values of the histogram for Z just between the G_1 and G_2 peak. The transition from S- to G_2-phase is principally the same, so we can take the same integral and only have to replace X_2 by X_4 and σ_2 by σ_4, respectively, and to change the integration limits. Thus, the S-phase curve has the form shown in Fig. 2A.

More than 50 DNA-histograms obtained from L-cells have been calculated to test the model. The "weighted variance" as introduced by Dean and Jett [3] was computed to indicate how well the data are described by the mathematical function used. The "weighted variance" is the sum of squares of the deviations divided by the number of counts (=square of the statistical error) and by the number of degrees of freedom. If the error of the data is exactly statistical and the function fits the data perfectly the weighted variance would be one. From the above-mentioned DNA-histograms the most carefully prepared and measured ones were selected *i.e.* those without cell debris and lumped cells [no counts below G_1-peak and above (G_2+ M)-peak]. For these samples we calculated weighted variances between 3 and 12 with an average of about 6. This agrees quite well with the weighted variance of 5 as given by Dean and Jett [3], though these authors have used a second degree polynomial to fit the S-region. The good agreement of the weighted variances shows that both approximations fit the data quite well.

In synchronized cell populations all cells enter S-phase at the same time. The distribution of the cellular DNA contents of S-cells can be assumed to be normal as well as for G_1 and (G_2+ M). In real experiments usually only a partial synchronization can be achieved. The more or less heavy contamination of non-synchronous cells leads to overlapping distributions [15]. If the proportion of synchronized cells is high (> 80%) the passage of the normal distributed cells through the S-phase can be clearly seen in the subsequent histograms [16]. The shape of the overlapping distribution of the contaminating cells depends on the method of synchronization. It will be different for agents synchronizing at different positions of the cell cycle. In our experiment cell cultures were synchronized by mechanical selection of mitotic cells [11]. During the passage of the synchronized subpopulation through the S-phase the DNA-histograms are of the type shown

in Fig. 2B. The peaks at the G_1- and (G_2 + M)-positions derive from the contaminating asynchronous cells. In this case the distribution of DNA contents of S-cells as well as those of G_1 and (G_2 + M) can be approximated by a normal distribution (see Fig. 2B). When the synchronized fraction reaches G_2-phase the histogram again shows only two peaks and model 2A has to be applied.

Based on the model described above, a computer program has been developed which chooses the proper version (A or B, Fig. 2). Version B is used if there is a peak between the G_1- and (G_2 + M)-peak, in all other cases version A is applied. The mathematical expressions for G_1-, S- and (G_2 + M)-phases are added up to a total function:

$$f(X) = G_1(X) + S(X) + G_2M(X) .$$

This function is fitted to the experimental histogram by the method of least squares. From the parameters (X_i, σ_i, C_i) obtained in the fit the fractions of cells in G_1-, S- and (G_2 + M)-phases are calculated taking the area under the corresponding curves related to the total area for all phases.

4. Results and Discussion

Fig. 3 shows a DNA-histogram obtained from Ehrlich ascites tumor cells in logarithmic growth. The cells have been taken from the peritoneal cavity of a grown-up mouse 6 days after inoculation. Determination of fractions of cells in the various phases of cell cycle with model 1 resulted in: G_1: 32%, S: 41%, (G_2 + M): 27%. The fraction of S-phase cells is relatively high, so the result is expected to contain a considerably high systematic error due to the approximation made in model 1. Another type of DNA-histogram is shown in Fig. 4, which was obtained from human bone marrow cells from a patient with acute lymphatic leukemia. In the original scale S- and (G_2 + M)-phase can hardly be seen, therefore these phases have been plotted again in an extended scale. Calculation with model 1 yielded: G_1: 90.6%, S: 7.7%, (G_2 + M): 1.7%. For this type of histograms model 1 is the appropriate one according to the above considerations.

Determination of fractions of cells in different phases with model 1 is very simple. If no computer is available, one can cut the areas of the corresponding phases out of the histogram to obtain the results by weighing. But for PCP-samples with high fractions of cells model 1 will introduce errors and for partially synchronized cell populations it cannot be applied at all.

In a previous investigation with L-929 cells in culture [17] cell cycle parameters obtained with autoradiographic and pulse-cytophotometric methods have been compared. The PCP-data were determined applying model 1. In the present work we have taken the same data but calculated the fractions of cells in the different phases using model 1 and model 2. Taking the total length of cell cycle from cell growth curves we calculated the length of G_1-, S- and (G_2 + M)-phases from the fractions of cells in these phases according to the method of Lennartz *et al.* [12]. The autoradiographic results have been determined using the labeled mitosis method of Quastler and Sherman [14]. In Table 1 are given the mean values of phase duration with standard errors of the mean obtained from five experiments. As can be seen from the Table, numerical values obtained with the two different models from PCP-data and with the autoradiographic methods are almost

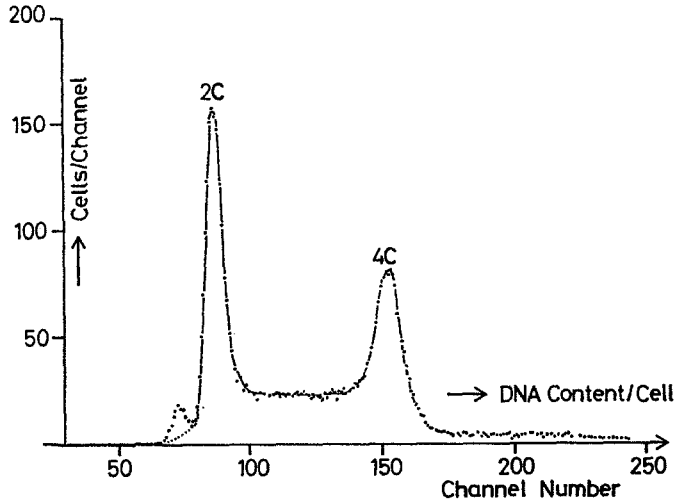

Fig. 3. Experimental DNA-histogram of Ehrlich ascites tumor cells. The abszissa is divided in 256 channels of a multi-channel analyzer corresponding to the DNA-content of the cells. On the ordinate the number of cells per channel is plotted, 100000 cells have been measured in 2 min. The small peak left of 2C originates from leucocytes with known DNA-content (6.5 pg/cell), it can be taken as a reference for the determination of the DNA-content of Ehrlich ascites cells

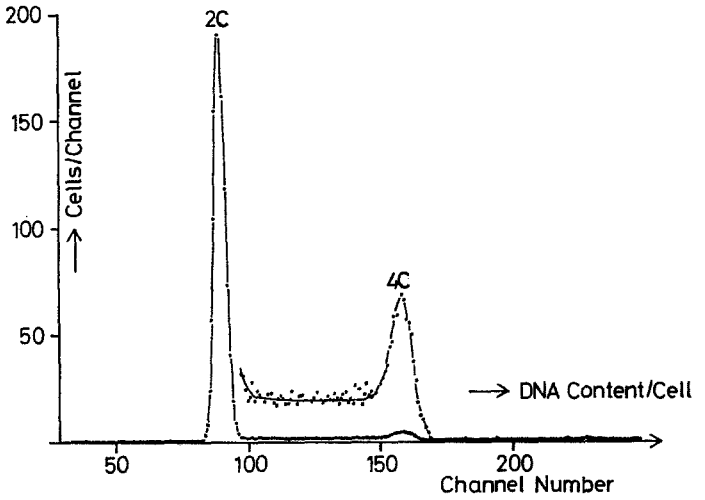

Fig. 4. Experimental DNA-histogram of human bone marrow cells from a patient with acute lymphatic leucemia, 98642 cells measured. On the right-hand part of the histogram the ordinate scale has been extended 16-fold (upper curve)

the same for all phases considered. This has been confirmed by a statistical test. The three mean values did not differ significantly from each other at the 5% level as performed by *t*-test. Comparing cell cycle parameters obtained by autoradiographic and PCP-methods it has to be pointed out that the number of measured

Table 1. Mean duration of phases of cell cycle for L-929-cells (hrs) with standard error of the mean (±)

Phase	Autoradiography	PCP (Model 1)	PCP (Model 2)
G_1	9.8 ± 2.7	10.6 ± 0.7	10.8 ± 0.7
S	7.7 ± 0.7	8.4 ± 0.4	9.0 ± 0.4
G_2 + M	5.5 ± 0.6	5.6 ± 0.4	4.8 ± 0.2
Total	23.0 ± 3.0	24.6 ± 1.3	24.6 ± 1.3

cells is some orders of magnitude higher using the PCP-method. Hence, the reproducibility is considerably better than with autoradiography as can be seen from the corresponding standard errors in Table 1. Thus the results obtained by PCP can be assumed to be more exact.

The mathematical analysis of PCP-data with the two models yields identical results for asynchronous cell populations. For cell populations with high fractions of S-phase cells model 2 has to be applied to get reliable results. In addition, errors from imperfect DNA-histograms, *i.e.* strong statistical deviations, cell debris or different cells as leucocytes in front of the G_1-peak (see Fig. 3), lumped cells appearing in channels following (G_2 + M)-peak, are eliminated or reduced by application of model 2. Thus, pulse-cytophotometry is a fast and powerful method for determination of cell cycle parameters provided an appropriate mathematical analysis is applied.

References

1. Charbit, A., Malaise, E. P., Tubiana, M.: Relation between the pathological nature and the growth rate of human tumors. Europ. J. Cancer **7**, 307—309 (1971)
2. Cleaver, J. E.: Thymidine metabolism and cell kinetics. In: Frontiers of biology, Vol. 6 (Neuberger, A., Tatum, P. L., *Eds.*). Amsterdam 1967
3. Dean, P. N., Jett, J. H.: Mathematical analysis of DNA distributions derived from flow microfluorometry. J. Cell Biol. **60**, 523—527 (1974)
4. Dittrich, W., Göhde, W.: Phase progression in two dose response of Ehrlich ascites tumour cells. Atomkernenergie **15—36**, 174—176 (1970)
5. Fabrikant, J. I., Cherry, J.: The kinetics of cellular proliferation in normal and malignant tissues. V. Analysis of labeling indices and potential tissue doubling times in human tumour cell populations. J. surg. Oncol. **1**, 23—34 (1969)
6. Göhde, W.: Zellzyklusanalysen mit dem Impulscytophotometer. Der Einfluß chemischer und physikalischer Noxen auf die Proliferationskinetik von Tumorzellen. Habilitationsschrift, Medizinische Fakultät, Münster 1973
7. Göhde, W., Dittrich, W.: Die cytostatische Wirkung von Daunomycin im Impulscytophotometrie-Test. Arzneimittel-Forsch. **21**, 1656—1658 (1971)
8. Göhde, W., Dittrich, W.: Impulsfluorometrie — Ein neuartiges Durchflußverfahren zur ultraschnellen Mengenbestimmung von Zellinhaltsstoffen. Acta histochem. (Jena) **10** (Suppl.), 429—437 (1971)
9. Göhde, W.: Automation of cytofluorometry by use of the Impulsmicrophotometer. In: Fluorescence techniques in cell biology, pp. 79—88 (Thaer, A. A., Sernetz, M., *Eds.*). Berlin-Heidelberg-New York: Springer 1973
10. Howard, A., Pelc, S. R.: Synthesis of DNA in normal and irradiated cells and its relation to chromosome breakage. Heredity **6** (Suppl.), 261—273, Symposium on Chromosome Breakage, Edinburgh (1953)

11. König, K., Linden, W. A., Canstein, M. v., Baisch, H., Canstein, L. v.: DNA-synthesis in synchronized L-cells after irradiation in the G_1-phase of the cell cycle. Rad. and Environm. Biophys. **12**, 23—30 (1975)
12. Lennartz, K. J., Maurer, W., Eder, M.: Auswertungsverfahren bei Doppelmarkierung mit C^{14}- und H^3-Thymidin für exponentielles Wachstum. Histochemie **13**, 84—90 (1968)
13. Madoc-Jones, H.: A review of the action of various chemotherapeutic agents on mammalian cells in the different phases of the cell generation cycle. Possible clinical implications. (In press)
14. Quastler, H., Sherman, F. G.: Cell population kinetics in the intestinal epithelium of the mouse. Exp. Cell Res. **17**, 420—438 (1959)
15. Rajewsky, M. F.: Synchronisation *in vivo*: Kinetics of a malignant cell system following temporary inhibition of DNA synthesis with hydroxyurea. Exp. Cell Res. **60**, 269—276 (1970)
16. Rajewsky, M. F., Grüneisen, A., Renner, I.: Modification of proliferative parameters by temporary inhibition of DNA synthesis. Studia biophysica **31/32**, 367—374 (1972)
17. Reddy, S. B., Erbe, W., Linden, W. A., Landen, H., Baigent, C.: Die Dauer der Phasen im Zellzyklus von L-929-Zellen. Vergleich von impulscytophotometrischen und autoradiographischen Messungen. Biophysik **10**, 45—50 (1973)
18. Sinclair, W. K.: Hydroxyurea: Differential lethal effects on cultured mammalian cells during the cell cycle. Science **150**, 1729—1731 (1965)
19. Sinclair, W. K.: Cyclic X-ray responses in mammalian cells *in vitro*. Radiat. Res. **33**, 620—643 (1968)
20. Tubiana, M.: The kinetics of tumour cell proliferation and radiotherapy. Brit. J. Radiol. **44**, 325—347 (1971)

Dr. H. Baisch
Institut für Biophysik
D-2000 Hamburg 20
Martinistr. 52
Federal Republic of Germany